Tectonophysics, 167 (1989) 41–55
Elsevier Science Publishers B.V., Amsterdam – Printed in The Netherlands

Seismotectonics and present-day relative plate motions in the New Hebrides–North Fiji Basin region

R. LOUAT and B. PELLETIER

ORSTOM U.R. A6, B.P.A5, Noumea Cedex (New Caledonia)

(Received October 7, 1988; revised version accepted January 31, 1989)

Abstract

Louat, R. and Pelletier, B., 1989. Seismotectonics and present-day relative plate motions in the New Hebrides–North Fiji Basin region. *Tectonophysics*, 167: 41–55.

Relative motions between the Pacific plate (P), Indo-Australian plate (IA), New Hebrides (NH) arc microplate and the North Fiji Basin (NFB) microplate are estimated using shallow seismicity, 276 focal mechanism solutions, bathymetry, magnetism and the RM-2 plate model of Minster and Jordan (1978).

Within the NFB, we define the western NFB (WNFB), eastern NFB (ENFB) and southern NFB (SNFB) microplates. A 8 cm/y spreading in a N72°E direction occurs along the N–S trending spreading ridge of NFB (WNFB–ENFB boundary). Along the ENFB–IA boundary located at 176°E, a 3 cm/y extension in a N108°E direction is proposed. The WNFB–P boundary which includes the Hazel Holme Extensional Zone (HHEZ), is complex and a general N25°E extension (2 cm/y) is inferred. The Fiji fracture zone (FFZ) is composed of two segments: Along the eastern zone (P–IA boundary) trending N80°E, a left-lateral strike-slip motion occurs (9.6 cm/y) accommodated by minor N109°E extension (pull-apart); while along the western zone (ENFB–P boundary) a N84°E trending left-lateral strike-slip motion (7 cm/y) is inferred. The WNFB–SNFB boundary corresponds to a N70°E broad fracture zone along which an E–W left-lateral strike-slip motion is proposed. The SNFB microplate moves rapidly eastwards (10.5 cm/y at 172°E) and is almost attached to the IA plate. Within the NFB, an improved model is discussed which includes deformations within the IA and P plates and rotations with Euler poles close to the NFB.

Along the New Hebrides trench, the consumption rates are respectively 16, 15, 9 and 12 cm/y at 11°, 12.5°, 15.5° and 20°S. The minimum rate occurs where the d'Entrecasteaux ridge collides with the New Hebrides arc. Rates of extension at the rear of the NH arc are 7, 5.5 and 2 cm/y at 11°, 12.5° and 20°S respectively. Back-arc compression occurs between 13°30′S and 17°S. The western end of the Hazel Holme extension zone coincides with the 13°30′S boundary separating the NH back-arc compressive belt and the northern NH back-arc troughs. South of 21°–22°S the trend of the slip vector changes along the NH trench from N70°E to N20°W. This implies a N–S motion of convergence along the E–W trending southern part of the NH trench (motion SNFB–IA of 1.5 cm/y at 172°E) and the existence of a N70°E trending left-lateral fracture zone crossing the southern part of the NFB. This fracture should be considered as a major plate boundary.

Introduction

In the southwest Pacific, converging motion along a part of the Pacific (P) and Indo-Australian (IA) plate boundary is accommodated by consumption of the IA plate along the New Hebrides (NH) and opening within the NH back-arc and the North Fiji Basin (NFB). Except Dubois et al. (1977), who quantified the consumption and extension rates in a global model, most authors focused their studies either on the NH subduction zone or on the NFB.

Along the New Hebrides trench, Isacks et al. (1981), Coudert et al. (1981) and Louat et al. (1988) estimated the direction of relative plate convergence (N70°–76°E). A rate of consump-

0040-1951/89/$03.50

tion of 12 cm/y has been calculated near 20°S by Dubois et al. (1977).

The NFB lying between the NH and Fiji Islands is recognized as a seismically active, complex and young (less than 10 M.y.) marginal basin (Sykes et al., 1969; Chase, 1971; Falvey, 1978; Halunen, 1979; Larue et al., 1982; Malahoff et al., 1982; Eguchi, 1984; Auzende et al., 1986a, b, 1988a, b; Lafoy et al., 1987; Pelletier et al., 1988; Hamburger and Isacks, 1988, in press; Kroenke et al., in press). Several models have been proposed concerning this present-day tectonics (Chase, 1971; Eguchi, 1984; Hamburger and Isacks, 1988; Auzende et al., 1988b; Pelletier and Louat, 1989). Although there is agreement on the location of the main active tectonic features within the NFB, based on marine survey and seismicity, directions of plate motions vary from model to model. For example, along the N–S spreading center in the central part of the NFB (NFBSC), Chase (1971) proposed a N96°E opening trend while Eguchi (1984) suggested an E–W or an NW–SE direction of opening. Recently Hamburger and Isacks (1988, in press) mapped the orientation of stressed within the NFB using focal mechanism solutions. Following these authors, it can be said that the lack of normal faulting solutions and the ubiquitous presence of strike-slip faulting mechanisms with fault planes oblique to the strike of the known topographic features do not demonstrate any simple system of regular spreading centers responsible for present-day extension, but indicate a diffuse and shear-dominated system of deformation in the NFB.

In this paper, we reconsider the present-day tectonics of the NFB and the directions of motions along the NH subduction zone and its back-arc domains using the shallow-seismicity distribution and an updated compilation of focal mechanism solutions.

Considering together the directions of motions (deduced from focal mechanisms) along each plate or microplate boundary (inferred from seismicity and/or morphology), the spreading rate along NFBSC (given by magnetic anomalies) and the IA-P motion (given by the model RM-2 of Minster and jordan, 1978), we propose a quantitative plate tectonic model of the NH–NFB region.

Data set

Figure 1 exhibits the distribution of epicenters of shallow earthquakes (depth 0–70 km) located by 20 or more world-wide seismological stations and obtained from the international Seismological Centre (ISC) catalog for the period 1964–1982 and from Preliminary Determination of Epicenters (PDE) monthly bulletins for the period 1983–1984. Earthquakes with magnitudes large enough to have a focal mechanism determination have been added for the period 1984–1987.

Focal mechanism solutions used in this study are issued from two data sets. The first data set (CMTS) is constituted by 267 moment tensor solutions for the 1977–1987 period. Events until March 1984 are obtained with the centroid moment tensor method (Dziewonski and Woodhouse, 1983; Dziewonski et al., 1983a, b, c; 1984a, b, c; 1987a, b, c; 1988a, b; Giardini et al., 1985) and events since April 1984 are solutions given by PDE monthly bulletins. The second data set (FMPS) is composed of nine first motion plane solutions from earthquakes located in the NFB for the period 1965–1976 (Sykes et al., 1969; Johnson and Molnar, 1972; Chinn and Isacks, 1983; Eguchi, 1984; Hamburger and Isacks, in press). Solutions from earthquakes for the period 1965–1976 related to the NH subduction zone have not been used because a large number of CMTS is available on this area.

Distribution of shallow seismicity and earthquake focal mechanisms

Three seismic domains are distinguished in the NH–NFB region. From west to east they are (Fig. 1): a densely-populated seismic belt west of the New Hebrides arc, a discontinuous but clearly-marked seismic belt along the eastern edge of the arc and a zone with diffuse seismic activity extending throughout the NFB.

Seismic belt west of the arc

This highly active seismic belt is related to the subduction of the IA plate under the NH arc. It strikes N160°E between the latitudes 21°S and

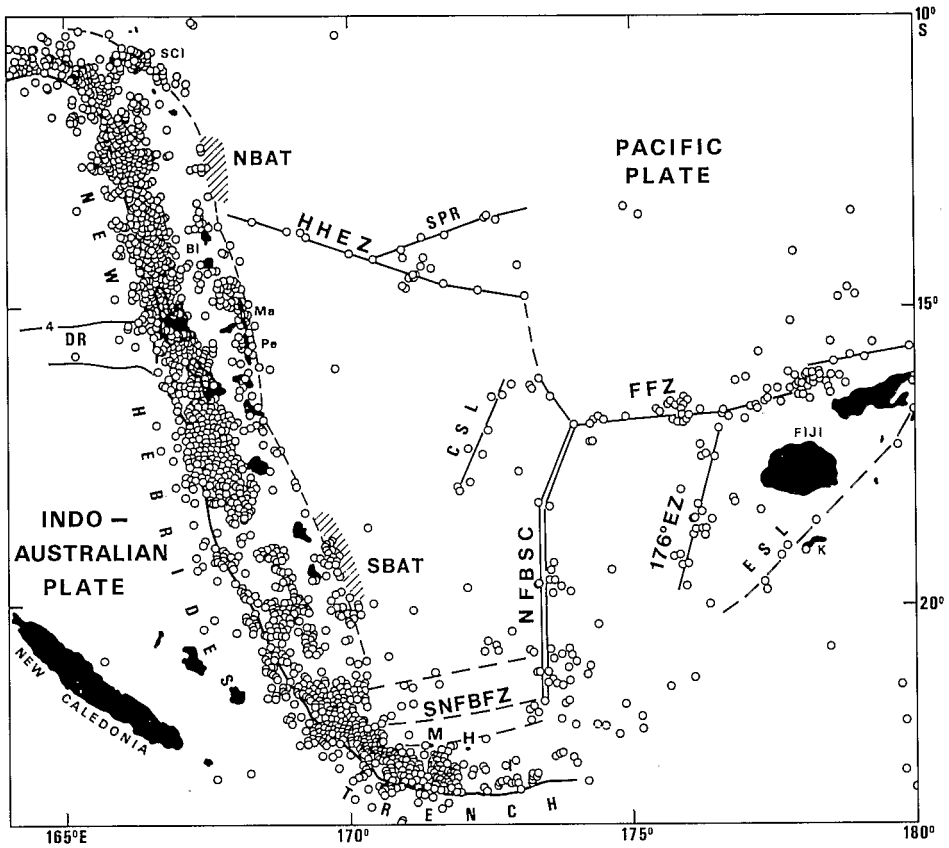

Fig. 1. Spatial distribution of shallow earthquakes (depth < 70 km) in the New Hebrides–North Fiji Basin region from 1964 to 1987, selected from ISC catalog (1964–1982), PDE Bulletins (1983–November 1984) and centroid moment tensor solution files (December 1984–1987). Plotted earthquakes are recorded by 20 stations or more. Boundaries of plates or microplates are shown. The spreading center in the central part of the North Fiji Basin (NFBSC) is represented by a double line. *HHEZ*—Hazel Holmes extensional zone (including *SPR*—South Pandora ridge); *FFZ*—Fiji fractures zone; *176°EZ*—176°E extensional zone; *SNFBFZ*—southern North Fiji Basin fracture zone. Hachured zones indicate New Hebrides back-arc trough areas: *NBAT*—northern back-arc troughs; *SBAT*—southern back-arc troughs. *SCI*—Santa Cruz islands; *BI*—Banks islands; *Ma*—Maewo island; *Pe*—Pentecost island; *M*—Matthew island; H—Hunter island; *K*—Kandavu island. *DR*—d'Entrecasteaux ridge; *CSL*—central seismic line; *ESL*—Eastern Seismic Line.

11°30′S, bends sharply westwards at the northern end of the arc, and turns progressively towards the east at its southern extremity. Trends of the nodal plane poles chosen as the direction of the slip vector of the interplate thrust-type focal mechanism solutions along the New Hebrides trench, are plotted on Fig. 2 and against the latitude of the epicenters on Fig. 3. Trends of the converging motion P–IA predicted by the RM-2 model of Minster and Jordan (1978) along the NH trench are also shown on Fig. 3. Two major areas can be identified along the NH trench: north of 21°S, slip vectors range N60–90°E in azimuth, while south of 21°S, slip vectors turn progressively from N60°E to N20°W in azimuth. The transition between these domains is characterized by a cluster of strike-slip solutions (Fig. 4). Between the latitudes 15° and 17°S the d'Entrecasteaux ridge collides with the arc. Here the trend of the slip vectors is close to E–W (N86°E) and parallels the direction of the motion IA–P predicted by the RM-2 model. In the northern extremity of the trench, the trends of slip vectors do not drastically change in spite of the westwards bending of the

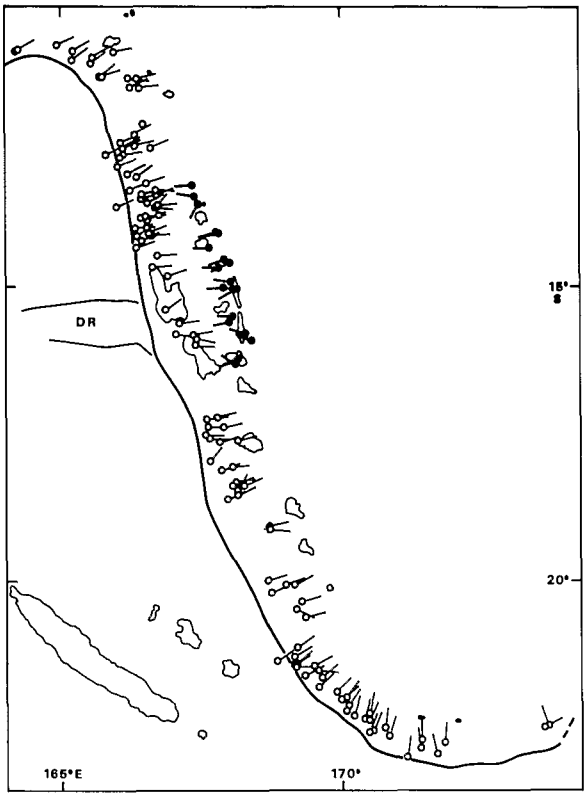

Fig. 2. Spatial distribution of epicenters of events with interplate thrust-type focal mechanism solutions (1977–1987) along the New Hebrides trench (open circles) and along the back-arc compressive belt (filled circles). Trends of the nodal plane poles taken as the direction of the slip motion are shown. Heavy line represents the New Hebrides trench axis. *DR*—d'Entrecasteaux ridge.

trench. Indeed, from 14°S to 10°S the average trend progressively changes from N72°E to N65°E.

Seismic belt east of the arc

Earthquakes are distributed along a discontinuous belt from 21°S to 10°S (Fig. 1). In detail, the back-arc area can be divided into three regions: a northern region from 10°S to 13°30′S, a central region between 13°30′S and 17°S and a southern region between 17°S and 21°S.

In the northern back-arc region, the seismicity, focal mechanisms and bathymetry allow the identification of three zones (Figs. 1 and 4):

(1) Numerous events cluster along a N120°E trending zone near 11°S, 166°30′E. This group coincides with a depression which separates islands belonging to the Santa Cruz archipelago. Three focal mechanisms indicate normal and strike-slip faulting. These solutions have a NE trending *T*-axis.

(2) At 10°20′S, 165°E, a N–S extension is indicated by a normal faulting and a strike-slip faulting solution sharing a common *T*-axis orientated N10°E.

(3) A small group of events can be observed at 12°30′S, 167°30′E along a N170°E trending zone. It is correlated with the Northern New Hebrides back-arc troughs (NBAT) newly mapped in detail by Récy et al. (1986) and Charvis and Pelletier (in press). Two events with normal faulting solutions are located just west of the troughs. They display a N125°E *T*-axis. This NW–SE direction disagrees with the NE–SW extension inferred by Seabeam data by (Charvis et Pelletier, in press).

In the central back-arc region, numerous earthquakes are distributed along a N170°E belt, extending from 13°30′S to 17°S, which bounds eastwards the NH central islands (Fig. 1). Twenty one focal mechanisms from earthquakes evenly distributed along this belt indicate thrust faulting. The morphology of the eastern flank of the island and the seismicity patterns suggest a west dipping thrust zone. Slip vectors from these thrust mechanisms range from N240°E to N280°E with a N265°E average trend. The *P*-axis strike from N110°E in the south to N60°E in the north (Figs. 2 and 4). At each extremity of this compressive belt, two events with strike-slip faulting solutions exist. The *P*-axis for these solutions strikes NE–SW in the north and ESE–WNW in the south. This back-arc compression has been documented already east of the Maewo and Pentecost islands and interpreted as a consequence of the d'Entrecasteaux ridge subduction (Collot et al., 1985). In fact back-arc compression extends over a distance of 400 km which is much larger than it was previous thought. This compressive belt largely overlaps northwards and southwards the portion of the arc located in front of the d'Entrecasteaux ridge (Fig. 4).

In the southern back-arc region, numerous events cluster between 18°50′S and 21°S along a

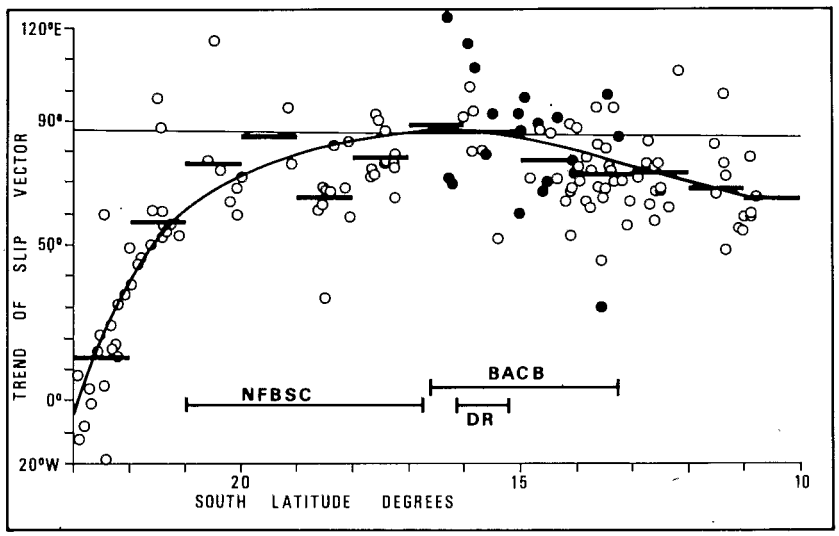

Fig. 3. Trends of slip vector from Fig. 2 plotted against latitudes of epicenters of events. Signification of open and filled circles same as Fig. 2. A smoothing curve is shown. Heavy segments represent the average trend for each degree of latitude. The straight line is the calculated slip vector azimuth of the relative motion between the Pacific and Indo-Australian plates along the trench using the RM-2 model of Minster and Jordan (1978). Geographical extension of some structures is shown; *NFBSC*—North Fiji Basin spreading center; *BACB*—back-arc compressive belt; *DR*—d'Entrecasteaux ridge.

N160°E trending zone which is located just west of the southern New Hebrides back-arc through (SBAT, Fig. 1). Along this belt, five normal faulting mechanisms documented a NE–SW extension (Fig. 4). Three of them are normal faulting solutions sharing a common N37°E *T*-axis (35, 37 and 38°E). This direction of extension is in good agreement with the N30°E extensional tectonics deduced from Seabeam data by Récy et al. (1986). In the southernmost end of the troughs, an earthquake with a strike-slip faulting solution showing a N73°E *T*-axis exists. In order to be coherent with the five previously-mentioned normal faulting solutions, we propose to interpret this latter solution as left-lateral strike-slip along a N27°E trending fault in N37°E regional extension.

Seismic activity in the North Fiji Basin (NFB)

Discrete zones of shallow seismicity within the NFB were first reported by Sykes et al. (1969). More recently, Hamburger and Isacks (in press) described in detailed the distribution of seismicity. As noted by these authors, earthquakes concentrate within certain areas delineating linear zones mainly associated with relatively shallow water areas. We consider that these diffuse seismic belts correspond to microplate boundaries. In this section, we will describe the seismicity and focal mechanisms along microplate boundaries using largely the well-documented analysis proposed by Hamburger and Isacks (in press).

The Fiji fracture zone (FFZ)

A sub E–W seismic belt (Fig. 1) extends from the north of Fiji platform (16°S, 180°E) to the triple junction located at 16°40′S, 174°E in the central part of the NFB (Lafoy et al., 1987). It represents the western part of a major lineament connected eastward to the northern closure of the Tonga trench. This lineament is the active Indo-Australian–Pacific plate boundary. In the area studied, the FFZ is composed of two segments (Fig. 1): the eastern one from 176°30′E to 180°E trends N80°E and is shifted at 178°E where numerous events cluster; the western segment extends from 176°30′E to 174°E and strikes N85°E. East of 176°30′E, the seismicity is correlated with narrow and linear structures bounding the north Fiji platform (cf. map from Auzende et al., 1988a). Other tectonic features located 100 km north of the FFZ and trending around N75°E

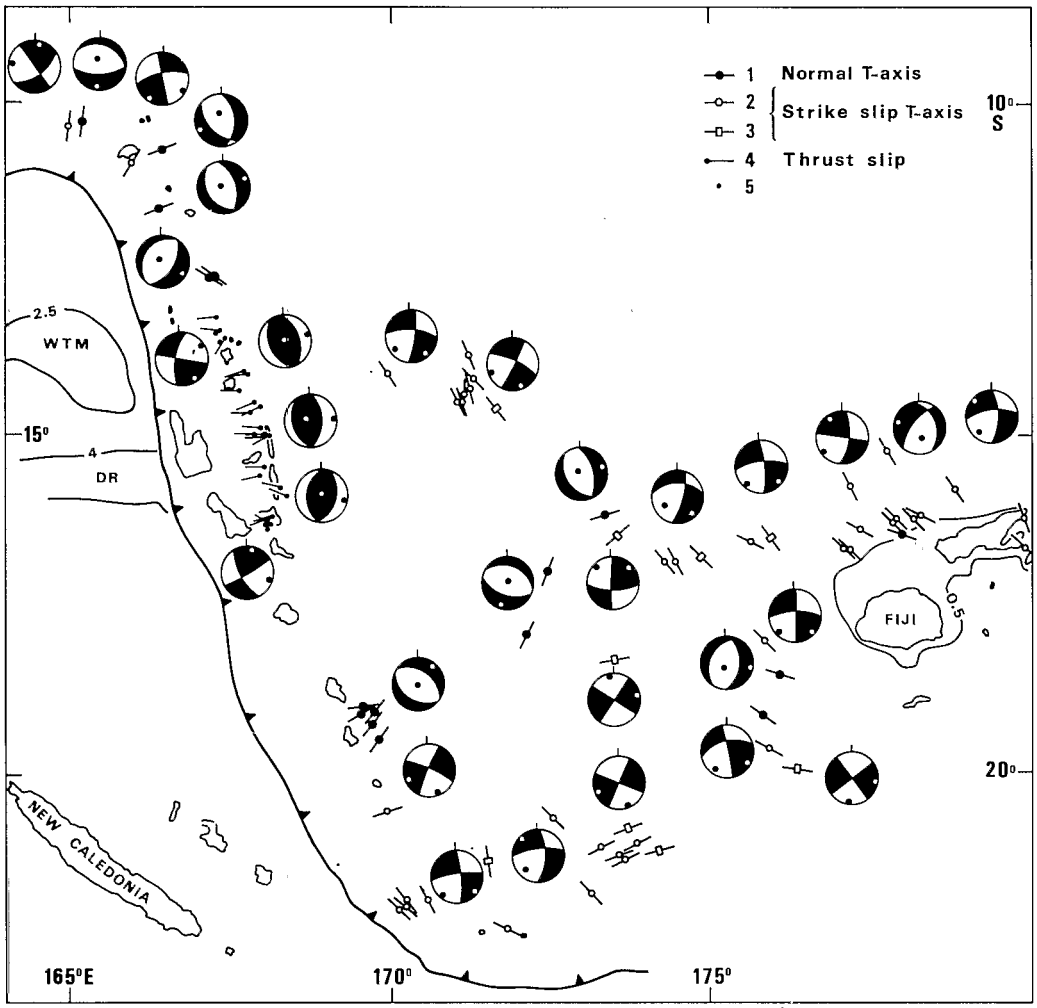

Fig. 4. Geographical compilation of focal mechanism solutions from shallow earthquakes (0–70 km) for the New Hebrides back-arc domain and the North Fiji Basin. Epicenters are represented by dots or squares. *T*-axes or slip vectors are shown by a line. *1* = *T*-axis associated with normal faulting solutions (CMTS); *2* = *T*-axis associated with strike-slip faulting solutions (CMTS); *3* = same as *2* for solutions from the period 1965–1976 (FMPS); *4* = slip vectors associated with back-arc thrust-type solutions (CMTS); *5* = epicenters of events with strike-slip faulting solutions associated with back-arc thrusting (CMTS). One focal sphere represents one or several similar solutions. Depth contours in km. *WTM*—West Torres massif; *DR*—d'Entrecasteaux ridge.

also coincide with few scattered events. West of 176°30′E, topographic expression of the FFZ is much more complex, including elements with various trends (Lafoy et al., 1987; Auzende et al., 1988a). Fifteen focal mechanisms, shown on Fig. 4, documented E–W trending left-lateral strike-slip motion along the FFZ as noted by previous authors (Sykes et al., 1969; Eguchi, 1984; Hamburger and Isacks, in press). At the place where the eastern segment is shifted (178°E), a cluster of earthquakes and one normal faulting solution with a N109°*E* *T*-axis are present. This solution bears on the existence of extension motion along the FFZ. This area is interpreted as a pull-apart basin along the left-lateral strike-slip FFZ. Morphological (N–S structures) and petrological (fresh basalt) evidences reported by Von Stackelberg (1985) also support this interpretation.

Hazel Holme extensional zone (HHEZ)

The HHEZ is delineated by discontinuous belt of seismicity extending from 14°S, 168°E to 15°S, 173°E. It crosscuts the northwestern part of the NFB up to the NBAT (Fig. 1). As noted by

Hamburger and Isacks (in press), this belt seems to relay the FFZ and to represent a segment of the active southern boundary of the Pacific plate. In detail the seismic belt has a "recumbent Y" shape and can be divided into three branches correlated with rough topography. These branches define a triple junction near 14°20°S, 170°30′E (Fig. 1):

(1) The northeastern branch trends N70°E and corresponds to the South Pandora ridge interpreted as a newly-created spreading center by Kroenke et al. (in press).

(2) The southeastern branch trends N95–100°E. It is associated with a N100°E morphological feature, and ends eastwards at 14°45′S, 173°E where Kroenke et al. (in press) proposed the existence of a relic ridge triple junction. The pattern of magnetic anomalies suggests that this branch in a sub-E–W spreading axis (Pelletier et al., 1988).

(3) The western branch trends N100–110°E and is located in the middle part of a 100 km wide active zone composed of horsts and grabens (Pelletier et al., 1988). This western branch ends just at the transition between the compressive back-arc belt and the NBAT.

Although morphology clearly indicates active tectonics of extension, no event with normal faulting solution exists along the HHEZ. Eight focal mechanism solutions along this structure indicate strike-slip faulting (Fig. 4). Six corresponding epicenters (including four from the November 1984 swarm) cluster along a NNE–SSW line near the 14°20′S, 170°30′E triple junction. All solutions have a nodal plane orientated around N25°E perpendicularly to the strike of the seismic belt. Consequently we propose that these mechanisms document NNE–SSW trending right-lateral strike-slip faulting in a N25°E opening tectonic context. A NE–SW direction of extension has also been inferred from a morphological and tectonic study of the NBAT and the western end of the HHEZ (Charvis et Pelletier, in press).

The main NFB active spreading center (NFBSC)

In the central part of the NFB, a spreading center has been identified between 16° and 21°S (Chase, 1971; Malahoff et al., 1982; Maillet et al., 1986; Auzende et al., 1986a, 1988a). The strike of the spreading axis is N–S between 21° and 18°10′S, N15°E between 18°10′ and 16°40′S then N160°E between 16°40′ and 16°S. The N15°E and N160°E axial ridges converge at 16°40′S with the western end of the FFZ, defining a triple junction (Lafoy et al., 1987; Auzende et al., 1988a). Along the well defined N–S segment, magnetic anomalies indicate a 6.8 to 8.2 cm/y full spreading rate for the last million years (Maillet et al., 1986; Auzende et al., 1988a). No continuous seismic belt correlates with the spreading axis. However, few clusters of events exist along it (Fig. 1). A major group of earthquakes occurs at the southern end of the axis near 21°S. Here a southward propagating rift and a N70°E transform fault have been inferred (Maillet et al., 1989). At this place, six similar focal mechanisms indicate strike-slip faulting solutions with a N65°E *T*-axis (Fig. 4). As noted by Hamburger and Isacks (in press), nodal planes are always orientated obliquely to the strike of the NFBSC. Another group of events appears near 19°40′S where a transverse structure and a change of the spreading rate for the last million years have been noted (Auzende et al., 1988a). At 18°20′S, close to the rift axis, Eguchi (1984) reports a strike-slip solution with a N79°E *T*-axis (Fig. 4). Lastly a few events are located at 16°20′S, 173°20′E, on the N160° E trending northwestern branch of the triple junction (Fig. 1). Two focal mechanisms document here (Fig. 4) normal faulting (N72°E *T*-axis) and strike-slip faulting (N50°E *T*-axis). We note that the *T*-axis of the normal fault solution is perpendicular to the strike of the rift mapped by Auzende et al. (1988a).

The 176°E extensional zone (176°EZ)

At 176°E a well-defined seismic belt trends N15°E between 17°S and 20°S (Fig. 1). It is associated with a rough topography composed of grabens and ridges striking respectively N15°E and N30°E north and south of 18°40′S (map from Auzende et al., 1988a). Along this zone, a young NNE–SSW spreading center has been postulated (Chase, 1971; Brocher and Holmes, 1985). More recently Auzende et al. (1986) interpreted the complex morphology of the area in terms of a tensional type deformation in a regional N45°E

left-lateral strike-slip system. Along this zone Hamburger and Isacks (in press) report one strike-slip fault solution. However, new computation of parameters of this focal mechanism gives a normal fault solution (Dziewonski et al., 1988a). Three additional focal mechanisms exist along this seismic belt (Fig. 4): one normal faulting solution and two strike-slip fault solutions. *T*-axes of the normal faulting solutions (N108°E and N126°E) are perpendicular to the strike of the grabens. As along the NFBSC, nodal planes of the strike-slip solutions are also orientated obliquely to the trend of the known topographic features.

Central seismic lineament (CSL)

A N25°E trending seismic line exists west of

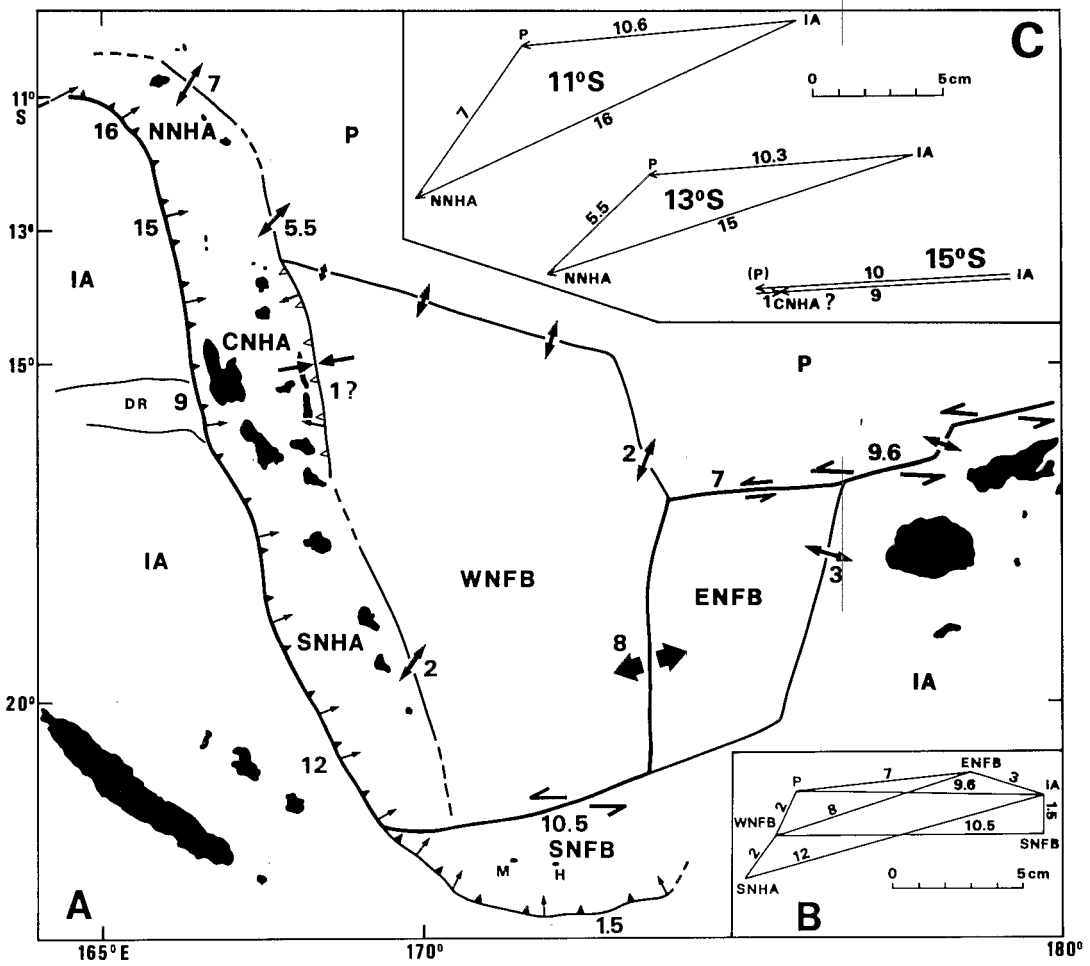

Fig. 5. Proposed quantitative model for present-day relative motions in the New Hebrides–North Fiji Basin region. A. Map showing the plate boundaries and the relative motions. *P*—Pacific plate; *IA*—Indo-Australian plate. *WNFB, ENFB* and *SNFB* represent respectively the western, eastern and southern North Fiji Basin microplates; *NNHA, CNHA* and *SNHA* are respectively the northern, central and southern segments of the New Hebrides arc microplate. Numbers and arrows beside plate boundaries indicate the rates and trends of the relative motions. Very thick divergent arrows show the motion along the main spreading center of the North Fiji Basin. Line with filled barbs corresponds to New Hebrides trench. Line with open barbs marks the New Hebrides back-arc compressive belt. DR—d'Entrecasteaux ridge; M and H—Matthew and Hunter islands. B. Vector diagram for motions in the North Fiji Basin. Vectors show motions of plates relative to the IA plate. Same legend as in A. C. Vector diagrams for motions along the New Hebrides arc at 11°S, 13°S and 15°S. Same legend as in A. The symbol (*P*) in the vector diagram at 15°S means that motion WNFB–P is assumed small enough to be ignored.

NFBSC between 16°20′S, 172°50′E and 18°10′S, 171°50′E (Fig. 1). The northern end of this line reaches the cluster of events associated with the northwestern branch of the triple junction. Two similar mechanisms illustrate normal faulting. *T*-axes of the solutions trend N28°E and N21°E. It is surprising to note that extensional stresses here are parallel to the strike of the seismic line.

Eastern seismic lineament (ESL)

A N50°E seismic line extends from 20°S, 177°E to the southern part of the Fiji platform (Fig. 1). It passes within the NFB more than 100 km north of the major depression extending from the eastern extremity of the NH trench to the south of Kandavu island. One mechanism from Johnson and Molnar (1972) exhibits strike-slip motion, which is left-lateral if the N45°E nodal plane is chosen (Fig. 4).

The southern NFB fracture zone (SNFBFZ)

A broad zone with diffuse seismicity showing possible N70°E trending lineations, exists in the southern NFB behind the arcuate termination of the New Hebrides arc (Fig. 1). This zone connects the NH arc with the southern extremity of the NFBSC. In this area, N70°E topographic features predominate (Maillet et al., 1989). Three similar focal mechanisms document strike-slip faulting (Fig. 4). These solutions have sub-E–W and N–S nodal planes and SE–NW *T*-axes. They indicate a left-lateral strike-slip motion if the E–W nodal planes are chosen as the fault. At 22°S within the NH trench-arc domain, five focal mechanisms have been obtained which are identical with the three previously mentioned (Fig. 4). A similar solution is also found just north of the Matthew Hunter islands. All these data support the existence of a diffuse N70°E fracture zone (SNFBFZ) acting as a left-lateral transform fault and extending from the south of the NH platform at 21–22°S to the southern end of the spreading axis at 21°S. Such a plate boundary is also needed to explain the rotation of the thrust motion from N75°E to N10°W along the southern NH trench. This rotation indicates a segmentation of the arc. In Fig. 5 only one plate boundary is drawn but the fracture zone appears complex and certainly includes several active tectonic lineaments.

Relative plate motions

Constraints on the plate tectonic model

According to the aforementioned data there exist the following constraints:

(1) The plate and microplate boundaries are inferred from the distribution of shallow seismicity (Figs. 1 and 4). In addition to the Pacific (P) and Indo-Australian (IA) plates, several microplates are postulated in the NFB (Fig. 5): the western NFB plate (WNFB), the eastern NFB plate (ENFB) and the southern NFB plate (SNFB). The New Hebrides arc is divided into three segments: the northern (NNHA), the central (CNHA) and the southern (SNHA) segments.

(2) The relative motion P–IA is given by the RM-2 model of Minster and Jordan (1978) assuming no intervening microplate motions.

(3) The direction of convergence along the NH trench is given by thrust-type solutions (Figs. 2 and 3).

(4) The 8 cm/y full spreading rate in a N72°E direction along the NFBSC is inferred from the pattern of magnetic anomalies proposed by Auzende et al. (1988a). The N72°E direction is deduced from five lines of evidence: (a) the strike-slip faulting mechanism with a N79°E *T*-axis near 18°30′S; (b) the cluster of six strike-slip faulting mechanisms with N65°E *T*-axis near 21°S at the southern tip of the spreading center; (c) the N80°E trending line linking the southern tips of the magnetic anomaly J present in both sides of the spreading center at 20°30′S (from figs. 4 and 8 of Maillet et al., 1989); (d) the set of transform faults orientated N70°E in the southwestern NFB; (e) the normal faulting mechanism with a N72°E *T*-axis just north of the triple junction.

(5) The N108°E direction of extension along the northern part of the 176°EZ is given by morphology and focal mechanisms.

(6) The N25°E direction of extension along the complex plate boundary in the northwestern part of the NFB (including HHEZ) is inferred from

morphology and focal mechanisms (see discussion before).

(7) The directions of extension in the NH back-arc domain are N37°E at 19°–20°S (SBAT), N45°E at 12°–13°S (NBAT) and N37°E at 10°–11°S. At 12°–13°S, two normal faulting solutions located just west of the troughs indicate a N125°E extension which is in disagreement with both the NE–SW extensional tectonics inferred from morphological study (Charvis et Pelletier, in press) and the azimuths of the slip vectors along the trench which are closer to the northern than those predicted by the RM-2 model (a back-arc extension in the trend given by those two mechanisms would imply a trend of the slip vector along the trench closer to the south). Thus these two solutions will not be considered in the model and we will adopt a N45°E extension in this area. At the northern extremity of the NH arc near the Santa Cruz islands (10°–11°S), normal and strike-slip faulting solutions have their *T*-axis perpendicular to the trench and orientated N65°E in the south and N10°E in the north (Fig. 4). The average direction of the *T*-axes (N37°E) is perpendicular to the N125°E trending back-arc seismic belt. Therefore a N37°E direction of extension in the back-arc area near 11°S has been used.

Results

Relative motions within the NFB

The constraints enable the construction of only one vector diagram. The plate motions are calculated relative to plate IA and are shown in Fig. 5 and Table 1. The motion P–IA is calculated at 17°S, 176°E using the RM-2 model of Minster and Jordan (1978). The proposed model is strongly reinforced by two observations: the direction of the left-lateral strike-slip motion ENFB–P (N264°E) is the same as the trend of the western seismic segment of the FFZ (N85°E); the consumption rate estimated here along the NH trench at 19–21°S (motion SNHA–IA: 12 cm/y), is the same as the subduction rate calculated by Dubois et al. (1977) from an associated lithospheric bulge of the IA plate. Within the NFB, we note that the largest relative motion is due to the main N–S spreading center. Other extensional zones (176°EZ, SBAT, HHEZ), along which relative motions are smaller, must be considered as second-order plate boundaries. The motion of the SNFB microplate is poorly constrained in comparison with other microplates. The value given in Table 1 is calculated at 172°E where the direction of the motion SNFB–IA is N–S. Between 21°S, 169°30′E and 23°S, 172°E the motion SNFB–IA varies progressively from 12 cm/y in an azimuth N255°E to 1.5 cm/y in an azimuth N180°E. The SNFB microplate is rapidly moving eastwards relatively to WNFB microplate and is almost attached to the IA plate. This explains that the eastern branch of boundary SNFB–IA is undefined by seismicity. Consequently the main plate boundary in the southern NFB region is not the southern part of the NH trench (SNFB–IA boundary) but a fracture zone located at 21°–22°S, north of the Matthew Hunter islands (WNFB–SNFB boundary). This boundary, termed the SNFBFZ, acts as a left-lateral transform fault accompanied with SE–NW extensional motion.

TABLE 1

Relative motions in the North Fiji Basin

Plate or microplate	Velocity (cm/y)	Azimuth (°E)
P–IA	9.6	271
ENFB–IA	3.0	288
ENFB–P	7.0	264
WNFB–ENFB	8.0	252
WNFB—P	2.0	205
SNHA–WNFB	2.0	217
SNHA–IA	12.0	255
SNFB–WNFB	10.5	90
SNFB–IA	1.5	180

The IA plate is assumed fixed and the motion P–IA is given at 17°S, 176°E by the RM-2 model of Minster and Jordan (1978). The motion SNFB–IA is given at 23°S, 172°E.

Relative motions along the New Hebrides trench and back arc

The results are reported in Fig. 5 and Table 2. North of the 21°–22°S boundary, the consumption rate varies along the NH trench from 12 cm/y in the southern part (18–21°S) to 15–16 cm/y in the northern part (11–13°S). The rate is

TABLE 2

Relative motions along the New Hebrides arc

Plate or microplate	Velocity (cm/y)	Azimuth (°E)	Latitude along the arc (°S)
NNHA–IA	16.0	245	
NNHA–P	7.0	217	11
P–IA	10.6	265	
NNHA–IA	15.0	252	
NNHA–P	5.5	225	13
P–IA	10.3	265	
CNHA–IA	9.0	266	
CNHA–WNFB	1.0	86	15
P–IA	10.0	266	
SNHA–IA	12.0	255	
SNHA–WNFB	2.0	217	20

The IA plate is assumed fixed and the motion P–IA is given by the RM-2 model of Minster and Jordan (1978).

minimum (9 cm/y) in front of the d'Entrecasteaux ridge where back-arc thrusting occurs (13°30–16°30'S). In this latter area, the average trend on the slip vector along both the trench and the back-arc compressive belt is the one predicted by the RM-2 model (N86°E, Fig. 3). This implies that the direction of resulting motion in the NFB at this latitude has to be close to N86°E. Such a direction of extension is unrealistic along the WNFB–P boundary because this would imply a right-lateral strike-slip motion along the HHEZ which is inconsistent with focal mechanisms. Topographic structures along WNFB–P also exclude a N86°E compression. Consequently we must conclude that, along the WNFB-P boundary, the N25°E extensional motion compatible with both tectonic features and focal mechanisms (2 cm/y in the model) vanishes towards the New Hebrides arc. In this scheme, the WNFB–P Euler pole is close to the HHEZ-arc junction, and the WNFB plate south of the western end of HHEZ is almost attached to the Pacific plate. Thus the consumption rate in front of the d'Entrecasteaux ridge may be deduced directly from the RM-2 model of Minster and Jordan (1978) which gives 10 cm/y. However this rate is lower because we have to consider some motion along the back-arc thrusting zone. As there are no data to quantify this motion, we have arbitrarily assigned 1 cm/y. This hypothesis gives in turn a consumption rate of 9 cm/y in front of the d'Entrecasteaux ridge (Fig. 5 and Table 2).

In the northern part of the NH arc, the calculated motion of extension within back-arc troughs is surprisingly high (5.5 cm/y at 13°S and 7 cm/y at 11°S). These values arise from the difference of 20° in azimuth between observed slip vectors along the trench and the ones predicted by the RM-2 model. Although the directions of extension in these troughs are not precisely constrained, seismicity, *T*-axes of focal mechanisms (with the exclusion of the two solutions previously mentioned) and bathymetry suggest that these directions are in a range N0°–70°E and turn from ENE to NNE going towards the north (Fig. 4). N–S and N70°E directions would imply respectively a 4 cm/y and an infinite rate of extension. At 13°S, the N45°E direction of back-arc extension (see before for justification) induces a 5.5 cm/y rate of extension. At 11°S the average trend of *T*-axes from all focal mechanism solutions is N37°E which results in a 7 cm/y rate of extension. These large rates of extension can be explained by additional stretching across northwestern part of the NFB, which creates seismically quiet horst and graben structures. Indeed, such an aseismic but tectonically active trough has been found inside the NFB just north of the HHEZ (Tikopia trough with fault scarps of 1500 m—Pelletier et al., 1988). The fast consumption rate in the northern extremity of the NH trench is compatible with the westwards curvature of the trench axis. The oceanic domain north of the West Torres massif (Fig. 4) is quickly vanishing in order to align the New Hebrides and the Solomon trenches.

Discussion of the model

A significant change of one of the parameters of the model (direction or velocity) drastically perturbs the relative motions which in turn would result in a disagreement with the data. Relative motions along the second-order boundaries (SBAT, 176°EZ and HHEZ) are directly dependent on the relative motion WNFB–ENFB along the main spreading center. In our model, the

selected N72°E direction of spreading is the best value considering the entire set of morphological and seismological data over the area. The N72°E direction is also the best value of minimize the relative velocities along the second order boundaries. The spreading direction cannot be reasonably outside the range N65°–80°E. When the value comes close N65°E, the relative velocity increases along the 176°EZ (4 cm/y), and HHEZ (2.5 cm/y), and diminishes in the SBAT (1.5 cm/y). If the direction passes beyond N65°E, then compression should occur in SBAT and the velocity of the extensional motion would be respectively 5 cm/y and 3 cm/y along the 176°EZ and the HHEZ. In contrast, when the spreading direction comes close to N80°E, the relative velocity increases along the SBAT (3 cm/y) and diminishes along the 176°EZ (2.5 cm/y) and the HHEZ (> 1 cm/y). If the direction is E–W, then compression should occur along the HHEZ and the rate of extension would be 2 cm/y along the 176°EZ and reach 5 cm/y in the SBAT.

Although the proposed model is coherent and accounts for most of the data, it can be improved if rotation and intraplate deformation are considered (Fig. 6). Within the NFB, relative plate motions described by close Euler poles fit with the data even better. Indeed, the observations favor rapid variations of velocity along some of the plate boundaries. Magnetic anomalies for example indicate that, along the N–S main spreading center, the full spreading rate is larger in the south

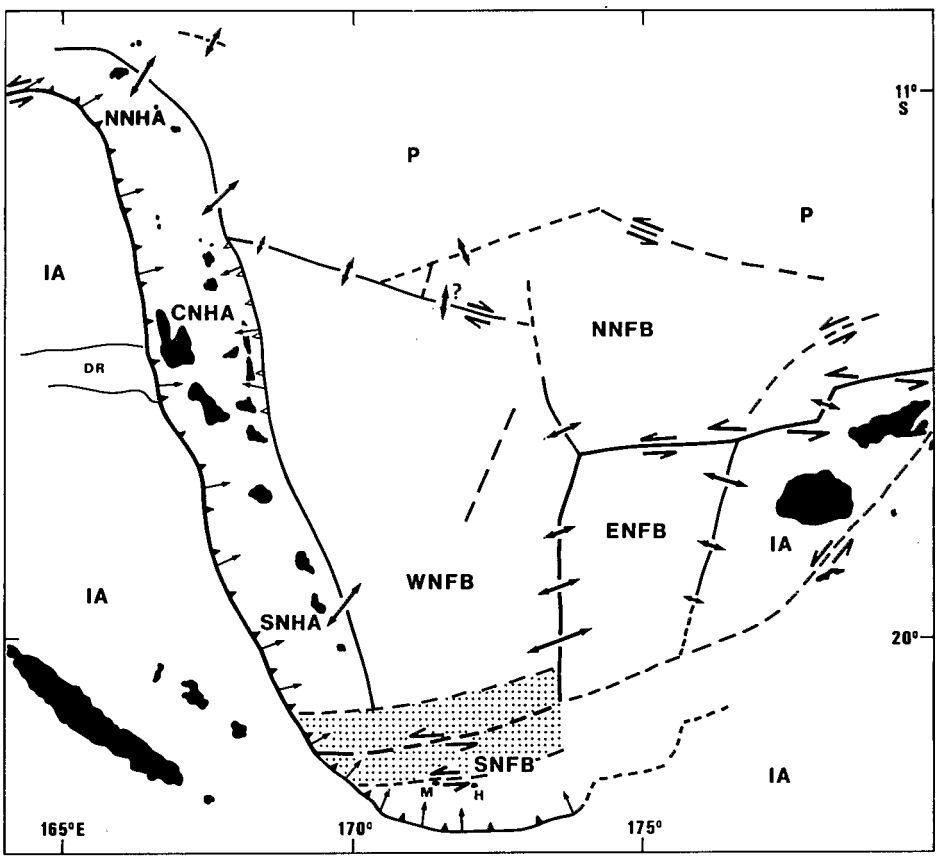

Fig. 6. Map showing plate and microplate boundaries and direction of motions in the study area, considering deformation within P and IA plates and relative motions between the North Fiji Basin microplates described by rotations with close Euler poles. Abbreviations and symbols are same as in Fig. 5. Arrows have no quantitative meanings. In this scheme, the northern North Fiji Basin plate (NNFB) is introduced. Discontinuous lines indicate seismically active zones along which stretching and/or shearing are inferred. Rotations are illustrated by arrows of different length along a same boundary. The dotted area corresponds to the inferred complex broad boundary between WNFB–SNFB.

than in the north (Auzende et al., 1988a). In the same way, the disappearance of seismicity at 20°S along the 176°EZ and the lack of a seismically-defined plate boundary in the south of the ENFB plate suggest that the motion of extension along the 176°EZ vanishes southwards. As noted before, the observed trend of the slip vector in front of the d'Entrecasteaux ridge and along the back-arc compressive belt implies that the rate of motion WNFB–P along the HHEZ decreases westwards. In conclusion, there is some evidence for rotations associated with close Euler poles, but the rotation parameters are difficult to quantify.

Intraplate deformation also plays a significant role within the NFB area. Indeed, some zones with seismic activity small enough to have been ignored in the global model, exist especially within the IA and P plates north and south of the FFZ (Fig. 1). Moreover, the important relative motions at the second order plate boundaries (176°EZ, HHEZ, SBAT and NBAT) can be largely reduced if we consider small left-lateral strike-slip motion within the P and IA plates along these diffuse seismic zones (Fig. 6). However, the deformation motion within the IA and P plates cannot exceed 2 cm/y because a decrease of the left-lateral strike-slip motion from 9.6 (RM-2 model) to 7.6 cm/y along the FFZ east of 176°E would imply no extension in SBAT, a small extensional rate (0.8 cm/y) along 176°EZ and a 2 cm/y extensional motion along HHEZ. The existence of a northern North Fiji Basin plate (NNFB, Fig. 6) bounded in the north by a left-lateral strike-slip fault provides a better explanation for the opening tectonics trend (N70°E) inferred by focal mechanisms and morphology along the N160°E branch of the 16°40′S–174°E triple junction. Presence of the NNFB plate also requires extension and right-lateral strike-slip motion along respectively the northeast (South Pandora ridge) and the southeast branches of the 14°20′S, 170°30′E triple junction. Opening tectonics along the South Pandora ridge have been proposed already by Kroenke et al. (in press). In any case, the direction of the resultant motion WNFB–P has to be close to N25°E (constraint in the western part of HHEZ). Because the NNFB–P motion is difficult to assess, we have not considered the existence of the NNFB in the quantitative model (Fig. 5), and a N25°E motion has been postulated along all the WNFB–P boundary.

Concluding remarks

The application of plate tectonics, even in an area as complex as the NFB evolving between the large P and IA plates, gives a coherent present-day model which successfully accounts for most of the marine as well as seismological data. The proposed model summarized in Figs. 5 and 6 and in Tables 1 and 2, although different, is not so far from the model proposed by Chase as soon as 1971. We must also emphasize that a ten years window of focal mechanism solutions computed with the centroid moment tensor method provides a coherent set of parameters which are in accordance with the morphotectonic structures. Seismotectonics using CMTS data is clearly a valuable and testable technique to accurately assess the directions of relative motions even in a complex area.

Acknowledgments

We are thankfull to J. Butscher for drafting the figures, to C. Baldassari for assistance in preparation of the data files and to J. Dupont, J. Daniel and M. Monzier for their critical reading of the manuscript. We are grateful to B.P. Luyendyk and one anonymous reviewer for reviewing the paper.

References

Auzende, J.M., Eissen, J.P., Caprais, M.P., Gente, P., Gueneley, S., Harmegnies, F., Lagabrielle, Y., Lapouille, A., Lefèvre, C., Maillet, P., Mazé, J.P., Ondréas, H., Schaaf, A. and Singh, R., 1986a. Accrétion océanique et déformation dans la partie méridionale du bassin Nord-Fidjien: résultats préliminaires de la campagne océanographique SEAPSO III du N.O. Jean Charcot (Décembre 1985). C.R. Acad. Sci. Paris, 303: 93–98.

Auzende, J.M., Lagabrielle, Y., Schaaf, A., Gente, P. and Eissen, J.P., 1986b. Tectonique intraocéanique déchrochante à l'ouest des îles Fidji (Bassin Nord-Fidjien). Campagne SEAPSO III du N.O. Jean Charcot. C.R. Acad. Sci. Paris, 303: 241–246.

Auzende, J.M., Eissen, J.P., Lafoy, Y., Gente, P. and Charlou,

J.L., 1988a. Seafloor spreading in the North Fiji Basin (Southwest Pacific). Tectonophysics, 146: 317–351.

Auzende, J.M., Lafoy, Y. and Marsset, B., 1988b. Recent geodynamic evolution of the North Fiji Basin (South West Pacific). Geology, 16: 925–929.

Brocher, T.M., and Holmes, R., 1985. The marine geology of sedimentary basins south of Viti Levu, Fiji. In: T.M. Brocher (Editor), Geological Investigations of the Northern Melanesian Borderland. Circum-Pac. Counc. Energy Miner. Resour. (Houston, Tex.), Earth Sci. Ser., 3: 123–138.

Charvis, P. and Pelletier, B., in press. The Northern New Hebrides back-arc troughs: history and relation with the North Fiji basin. Tectonophysics.

Chase, C.G., 1971. Tectonic history of the Fiji Plateau. Geol. Soc. Am. Bull., 82: 3087–3110.

Chinn, D.S. and Isacks, B.L., 1983. Accurate source depths and focal mechanism of shallow earthquakes in western South America and in the New-Hebrides island arc. Tectonics, 2(6): 529–563.

Collot, J.Y., Daniel, J. and Burne, R.V., 1985. Recent tectonics associated with the subduction/collision of the d'Entrecasteaux zone in the central New Hebrides. Tectonophysics, 112: 325–356.

Coudert, E., Isacks, B.L., Barazangi, M., Louat, R., Cardwell, R., Chen, A., Dubois, J., Latham, G. and Pontoise, B., 1981. Spatial distribution and mechanisms of earthquakes in the southern New-Hebrides arc from a temporary land and ocean bottom seismic network and from worldwide observations. J. Geophys. Res., 86: 5905–5925.

Dubois, J., Launay, J., Récy, J. and Marshall, J., 1977. New Hebrides trench: subduction rate from associated lithospheric bulge. Can. J. Earth. Sci., 14: 250–255.

Dziewonski, A.M. and Woodhouse, J.H., 1983. An experiment in systematic of global seismicity: Centroid-moment tensor solutions for 201 moderate and large earthquakes of 1981. J. Geophys. Res., 88 (B4): 3247–3271.

Dziewonski, A.M., Friedman, A., Giardini, D. and Woodhouse, J.H., 1983a. Global seismicity of 1982: Centroid moment tensor solutions for 308 earthquakes. Phys. Earth Planet. Inter., 33: 76–90.

Dziewonski, A.M., Friedman, A. and Woodhouse, J.H., 1983b. Centroid-moment tensor solutions for January–March, 1983. Phys. Earth Planet. Inter., 33: 71–75.

Dziewonski, A.M., Franzen, J.E. and Woodhouse, J.H., 1983c. Centroid-moment tensor solutions for April–June, 1983. Phys. Earth Planet. Inter., 33: 243–249.

Dziewonski, A.M., Franzen, J.E. and Woodhouse, J.H., 1984a. Centroid-moment tensor solutions for July–September, 1983. Phys. Earth Planet. Inter., 34: 1–8.

Dziewonski, A.M., Franzen, J.E. and Woodhouse, J.H., 1984b. Centroid-moment tensor solutions for October–December, 1983. Phys. Earth Planet. Inter., 34: 129–136.

Dziewonski, A.M., Franzen, J.E. and Woodhouse, J.H., 1984c. Centroid-moment tensor solutions for January–March, 1984. Phys. Earth Planet. Inter., 34: 209–219.

Dziewonski, A.M., Ekström, G., Franzen, J.E. and Woodhouse, J.H., 1987a. Global seismicity of 1977: Centroid-moment tensor solutions for 471 earthquakes. Phys. Earth Planet. Inter., 45: 11–36.

Dziewonski, A.M., Ekström, G., Franzen, J.E. and Woodhouse, J.H., 1987b. Global seismicity of 1978: Centroid-moment tensor solutions for 512 earthquakes. Phys. Earth Planet. Inter., 46: 316–342.

Dziewonski, A.M., Ekström, G., Franzen, J.E. and Woodhouse, J.H., 1987c. Global seismicity of 1979: Centroid-moment tensor solutions for 524 earthquakes. Phys. Earth Planet. Inter., 48: 18–46.

Dziewonski, A.M., Ekström, G., Franzen, J.E. and Woodhouse, J.H., 1988a. Global seismicity of 1980: Centroid-moment tensor solutions for 515 earthquakes. Phys. Earth Planet. Inter., 50: 127–154.

Dziewonski, A.M., Ekström, G., Franzen, J.E. Woodhouse, J.H., 1988b. Global seismicity of 1981: Centroid-moment tensor solutions for 542 earthquakes. Phys. Earth Planet. Inter., 50: 155–182.

Eguchi, T., 1984. Seismotectonics of the Fiji Plateau and Lau Basin, Tectonophysics, 102: 17–32.

Falvey, D.A., 1978. Analysis of paleomagnetic data from the New Hebrides. Bull. Aust. Soc. Explor. Geophys., 9 (3): 117–123.

Giardini, D., Dziewonski, A.M. and Woodhouse, J.H., 1985. Centroid-moment tensor solutions for 113 large earthquakes in 1977–1980. Phys. Earth Planet. Inter., 40: 259–272.

Halunen, A.J., 1979. Tectonic history of the Fiji plateau. Unpublished PhD. Honolulu, Hawaii, 127 pp.

Hamburger, M.W. and Isacks, B.L., 1988. Diffuse back-arc deformation in the southwestern Pacific. Nature, 332: 599–604.

Hamburger, M.W. and Isacks, B.L., in press. Shallow seismicity in the North Fiji basin. In L.W. Kroenke and J.V. Eade (Editors), Geological Investigations of the North Fiji Basin: Circum-Pac. Counc. Energy Miner. Resour. (Houston, Tex.), Earth Sci. Ser.

Isacks, B.L., Cardwell, R.K., Chatelain, J.L., Barazangi, M., Marthelot, J.M., Chinn, D. and Louat, R., 1981. Seismicity and tectonics of the central New-Hebrides island arc. In: D.W. Simpson and P.G. Richards (Editors), Earthquake Prediction: An International Review. Am. Geophys. Union, Maurice Ewing Ser., 4, pp. 93–116.

Johnson, T. and Molnar, P., 1972. Focal mechanisms and plate tectonics of the Southwest Pacific. J. Geophys. Res., 77: 5000–5032.

Kroenke, L.W., Jouannic, C. and Woodward, P., 1983. Bathymetry of the Southwest Pacific, chart I of the Geophysical Atlas of the South West Pacific. United Nations ESCAP, CCOP/SOPAC, scale 1: 6442192.

Kroenke, L.W., Smith, R. and Nemoto, K., in press. Geomorphology and crustal of the North Fiji Basin. In: L.W. Kroenke and J.V. Eade (Editors), Geological Investigations of the North Fiji Basin. Circum-Pac. Counc. Energy Miner. Resour. (Houston, Tex.), Earth Sci. Ser.

Lafoy, Y., Auzende, J.M., Gente, P. and Eissen, J.P., 1987. L'extrémité occidentale de la zone de fracture fidjienne et le point triple de 16°40S. Résultats du leg III de la campagne SEAPSO du N.O. Jean Charcot (décembre 1985) dans le bassin Nord Fidjien, SW pacifique. C.R. Acad. Sci., Paris, 304: 147–152.

Larue, B.M., Pontoise, B., Malahoff, A., Lapouille, A. and Latham, G.V., 1982. Bassins marginaux actifs du sud-ouest Pacifique: Plateau Nord-Fidjien, Bassin de Lau. Trav. Doc. ORSTOM, 147: 363–406.

Louat, R., Hamburger, M. and Monzier, M., 1988. Shallow and intermediate-depth seismicity in the New Hebrides arc: Constraints on the subduction process. In: H.G. Greene and F.L. Wong (Editors), Geology and Offshore Resources of Pacific Islands Arcs—Vanuatu region. Circum-Pac. Counc. Energy Miner. Resour. (Houston, Tex.), Earth Sci. Ser. 8: 329–356.

Maillet, P., Eissen, J.P., Lapouille, A., Monzier, M., Baleivanualala, V., Butscher, J., Gallois, F. and Lardy, M., 1986. La dorsale active du bassin Nord-Fidjien entre 20,00°S et 20,53°S: signature magnétique et morphologie. C.R. Acad. Sci., Paris, 302: 135–140.

Maillet, P., Monzier, M., Eissen, J.P. and Louat, R., 1989. Geodynamics of an arc–ridge junction: the New Hebrides Arc/North Fiji Basin case, Tectonophysics, 165: 251–268.

Malahoff, A., Feden, R.H. and Fleming, H.F., 1982. Magnetic anomalies and tectonic fabric of marginal basins north of New Zealand. J. Geophys. Res., 87: 4109–4125.

Minster, J.B. and Jordan, T.H., 1978. Present day plate motions. J. Geophys. Res., 83: 5331–5354.

Pelletier, B. and Louat, R., 1989. Mouvements relatifs des plaques dans le Sud-Ouest Pacifique. C.R. Acad. Sci. Paris, 308: 123–130.

Pelletier, B., Charvis, P., Daniel, J., Hello, Y., Jamet, F., Louat, R., Nanau, P. and Rigolot, P., 1988. Structure et linéations magnétiques dans le coin Nord-Ouest du bassin Nord-Fidjien: résultats préliminaires de la campagne Eva 14 (août 1987). C.R. Acad. Sci. Paris, 306, II: 1247–1254.

Récy, J., Charvis, P., Ruellan, E., Monjaret, M.C., Gerard, M., Auclair, G., Baldassari, C., Boirat, J.M., Brown, G.R., Butsher, J., Collot, J.Y., Daniel, J., Monzier, M. and Pontoise, B., 1986. Tectonique et volcanisme sousmarin à l'arrière de l'arc des Nouvelles-Hébrides (Vanuatu, Pacifique Sud-Ouest): résultats préliminaires de la campagne SEAPSO leg III du N/O Jean Charcot. C.R. Acad. Sci., Paris, 303: 685–690.

Sykes, L.R., Isacks, B.L. and Oliver, J., 1969. Spatial distribution of deep and shallow earthquakes of small magnitudes in the Fiji–Tonga region. Bull. Seismol. Soc. Am., 59: 1093–1113.

Von Stakelberg, U. and the Shipboard Scientific Party of Sonne Cruise SO-35, 1985. Hydrothermal sulfide deposit in back-arc spreading centers in the Southwest Pacific. Bundesanst. Geowiss. Rohstoffe, Circ., 2: 14 pp.